The Hydrophobic Effect Contributes to Polyubiquitin Chain Recognition†

Richard E. Beal,‡ David Toscano-Cantaffa,‡ Patrick Young,§ Martin Rechsteiner,§ and Cecile M. Pickart*,‡

Department of Biochemistry, School of Public Health, Johns Hopkins University, Baltimore, Maryland 21205, and Department of Biochemistry, University of Utah School of Medicine, Salt Lake City, Utah 84132

Received October 10, 1997

ABSTRACT: The principal targeting signal used in the ubiquitin−proteasome degradation pathway is a homopolymeric, K48-linked polyubiquitin chain: the chain is recognized by a specific factor(s) in the 19S regulatory complex of the 26S proteasome, while the substrate is degraded by the 20S catalytic complex. We have previously presented evidence implicating the side chains of L8, I44, and V70 in the recognition of K48-linked chains. In the crystal structure of tetraubiquitin, these side chains form a repeating, surface-exposed hydrophobic patch. To test the hypothesis that a close-packing interaction involving this patch is important for the chain recognition, residue 8 was mutated to a series of smaller aliphatic amino acids (G, A, V). The effects of these mutations were first investigated in rabbit reticulocyte fraction II; even the severest truncating mutation (L8G) had only a modest inhibitory effect on the degradation of a model substrate (^{125}I-lactalbumin). We show that these steady-state degradation data substantially underestimate the deleterious effects of these mutations on chain recognition by the proteasome, because the recognition step does not contribute to rate limitation in the fraction II system. Much stronger inhibition was observed when chain binding was measured in a competition assay using purified 26S proteasomes, and the change in binding free energy depended linearly on the surface area of the side chain. This behavior is consistent with a mode of binding in which the hydrophobic effect makes a favorable contribution; i.e., one or more L8 side chains is shielded from solvent when the chain binds to the 19S complex. A similar linear dependence of binding energy on side chain area was observed for chain binding to the 19S subunit known as S5a (as assayed using recombinant S5a bound to nickel beads). Octa-ubiquitin ($K_{0.5}$ = 1.6 μM) bound to S5a 4.2-fold more tightly than tetra-ubiquitin; this is similar to the factor of 5.8-fold relating the affinities of the same two chains for the 26S proteasome. Altogether, these findings indicate that the interaction of K48-linked chains with the 19S complex is substantially similar to the interaction of chains with isolated S5a. The results further suggest that the hydrophobic patch is part of a minimum element which allows for specific recognition of the polyubiquitin degradation signal by the 26S proteasome.

The ubiquitin−proteasome pathway is the principal mechanism for the turnover of short-lived proteins in eukaryotic cells (*1*−*3*). In this essential pathway, the conserved polypeptide ubiquitin acts as a degradation signal by virtue of covalent linkage to cellular substrates. This is accomplished through the formation of an isopeptide bond between the C-terminus of ubiquitin (G76) and an internal Lys residue of the substrate. Formation of the ubiquitin−substrate bond is usually followed by further rounds of conjugation involving K48 of ubiquitin itself, which lead to the assembly of a long polyubiquitin chain. Although the ligation of a single ubiquitin can target a substrate for degradation (*4*, *5*), K48-linked chains apparently represent the predominant signal for targeting substrates to the 26S proteasome. This is indicated both by the unique lethality of the K48R mutation in yeast (*6*, *7*) and by the finding that that a substrate bearing a homopolymeric K48-linked chain is degraded by the 26S proteasome much faster than a mono-ubiquitinated form of the same substrate (*8*, *9*). Polyubiquitin chains linked through other Lys residues of ubiquitin have also been observed (*7*, *10*, *11*), but as yet their functions are poorly understood.

The 26S proteasome is formed by the assembly of the 20S proteasome with a second complex known as the 19S regulatory complex or PA700 (*12*, *13*). The 700-kDa 20S complex contributes the catalytic machinery to the 26S proteasome. The 20S proteasome consists of 28 subunits that form a cylindrical array, and its proteolytic active sites line an interior chamber that is too narrow to accommodate a folded protein (*14*, *15*). In accord with this architecture, the substrates of the isolated 20S proteasome are restricted to small peptides and denatured proteins; activity toward ubiquitin-conjugated proteins is realized only upon assembly of the 20S and 19S complexes (two 19S complexes assemble with one 20S proteasome). The assembly reaction and the degradation of ubiquitin conjugates are both ATP-dependent processes.

† This work was supported by NIH Grant DK46984 (to C.M.P.), and NIH Grant GM37009 and the Lucille P. Markey Charitable Trust (to M.R.). This work is in partial fulfillment of the Ph.D. and M.S. degrees in Biochemistry to R.E.B. and D.T.C., respectively, from the State University of New York at Buffalo.

* Address correspondence to this author at the Department of Biochemistry, Johns Hopkins University, 615 N. Wolfe St., Baltimore, MD 21205. Telephone: (410) 614-4554. Fax: (410) 955-2926. E-mail: cpickart@welchlink.welch.jhu.edu.

‡ Johns Hopkins University.

§ University of Utah School of Medicine.

S0006-2960(97)02514-2 CCC: $15.00
Published on Web 02/14/1998

The 700-kDa 19S complex consists of about 20 subunits, most of which are functionally uncharacterized (*16*). Activities expected to reside in this complex include polyubiquitin recognition, substrate unfolding, and possibly ubiquitin/polyubiquitin removal. Among the 19S subunits are six proteins which belong to the ATP-binding cassette protein family (see *3*, *17*, *18*). These subunits may be required for substrate unfolding, or for maintaining the association between the 19S and 20S complexes. Another subunit of the 19S complex has deubiquitinating activity, and may serve an editing function (*5*). Yet another subunit, known as S5a, MBP1, or Mcb1p, binds polyubiquitin chains, consistent with a role in chain recognition (*11*, *19*, *20*). The substantial proteolytic competence of the *mcb1*Δ yeast strain (*21*) indicates that additional chain-binding subunits must be present in the 19S complex.

We recently showed that K48-linked Ub_8[1] binds to the 26S proteasome 90 times more tightly than Ub_2, providing a quantitative indication of the degree to which assembly into a chain potentiates ubiquitin's targeting ability (*22*). We suggested that a K48-linked polyubiquitin chain is an efficient degradation signal due to the presence of multiple copies of a minimal recognition element on the chain surface. One candidate component of this element is a hydrophobic patch composed of the side chains of L8, I44, and V70. This patch is a repeating, surface-exposed feature in the crystal structure of Ub_4 (*23*), and its component side chains are demonstrably important for function: chains assembled from L8A,I44A-ubiquitin do not bind detectably to the proteasome or to isolated S5a (*24*). A reasonable explanation for the deleterious effect of the L8A,I44A double mutation assumes that the L8A and I44A side chains are shielded from solvent when chains bind to the proteasome or S5a. This binding mode would enjoy a favorable entropic contribution from the hydrophobic effect, which would be reduced (as observed) upon decreasing the side chain surface area by mutation to Ala.

To test whether recognition of polyubiquitin chains involves a close-packing interaction with L8, we made a series of mutant ubiquitins in which L8 was replaced by aliphatic amino acids with smaller side chains. If this side chain is shielded from solvent when polyubiquitin chains bind to their recognition element(s), the predicted outcome is a graded change in binding energy that is directly proportional to the change in side chain surface area (*25*, *26*). We show that chain binding to isolated S5a conforms to this prediction. Data obtained with the 26S proteasome, while more limited, suggest a similar dependence. These and other results are consistent with the mode of binding discussed above, and suggest that the interaction of chains with the 26S proteasome is substantially similar to the interaction of chains with isolated S5a.

EXPERIMENTAL PROCEDURES

Ubiquitin Plasmids. Mutant ubiquitins were expressed using the IPTG-inducible pET3a vector. Genes encoding the following ubiquitins were moved from pPLhUb (*24*, *27*) into pET3a: wild-type; L8A; I44A; and L8A,I44A. This was accomplished by amplifying the coding sequences, using the appropriate pPLhUb vector as template, with primers Ub5F (5′-tgcatttatttgcatacattca-3′) and Ub3F (5′-cgaattc-gagctcggatcctcaa-3′). The PCR products were digested with *Nde*I and *Bam*HI, and subcloned into *Nde*I/*Bam*HI-digested pET3a. Plasmids encoding L8I−, L8V−, L8G−, and L8W−ubiquitin were generated by a two-step PCR method using pPLhUb as template (*28*). The first-stage PCR utilized primer Ub5F and one of the following mutagenic primers: 5′-accggttatcgtcttgac-3′ (L8I); 5′-accggttaccgtcttgac-3′ (L8V); 5′-accggttcccgtcttgac-3′ (L8G); 5′-accggtccacgtcttgac-3′ (L8W). In each case, the first-stage PCR product was purified, and used as the 5′ primer in the second-stage PCR with Ub3F as the 3′ primer. The second-stage PCR products were digested with *Nde*I and *Bam*HI, and cloned into pET3a. All coding regions were sequenced (fmol kit, Promega).

Ubiquitin Expression and Purification. Wild-type and mutant ubiquitins specified by pET3a plasmids were expressed in *E. coli* strain BL21(DE3)pLysS following induction with IPTG; induction, cell lysis, and ubiquitin purification were as described (*22*).

Polyubiquitin Chain Synthesis and Purification. Recombinant bovine E2-25K was purified as described (*29*, *30*). E1 was purified as described (*31*). Mixtures of K48-linked polyubiquitin chains were synthesized as described previously (*29*), except that the pH was 8.0. Incubations (37 °C) contained 0.2 μM E1, 10 μM E2-25K, and 2 mg/mL ubiquitin. The incubation time was adjusted (20−60 min) to provide a comparable length distribution of chains in each case (*n* ranging from 1 to ∼6; see Figure 3A, Results). The enzymes were absorbed onto anion-exchange resin (*29*). The chains were first concentrated by ultrafiltration to ∼200 μL, and then concentrated further using a speed-vac at ambient temperature.

Protein Radioiodination. Bovine lactalbumin (Sigma), mixed polyubiquitin chains (above), and homogeneous Ub_4 and Ub_8 (*22*) were radioiodinated with chloramine T (*32*). Typical reactions contained 100 μg of protein and 100−200 μCi of carrier-free $Na^{125}I$ (Amersham) in a volume of 50−100 μL. Labeled proteins were separated from unincorporated label on Sephadex G-25 spin columns. Specific radioactivity was typically $(0.5-1) \times 10^6$ cpm/μg.

Protein Degradation and Conjugate Levels in Reticulocyte Fraction II. The ability of mutant ubiquitins to support the degradation of ^{125}I-lactalbumin, and to support conjugation in the degradative steady-state, was determined at 37 °C in incubations containing (*24*) 50 mM Tris-HCl (pH 7.3), 5 mM $MgCl_2$, 2 mM ATP, 1 mM DTT, an ATP-regenerating system, rabbit reticulocyte fraction II protein (*32*) at 1 mg/mL, ^{125}I-lactalbumin at 5 μg/mL (∼300 nM), and ubiquitin at 12 μM. For degradation, the production of acid-soluble radioactivity was monitored at times ranging from 5 to 40 min (Results). Assays were initiated with the labeled substrate following a 4-min preincubation of all other components at 37 °C. The data were corrected by subtracting blanks derived from incubations lacking ubiquitin, and results were expressed relative to a control containing wild-type ubiquitin. To measure conjugate levels, aliquots of the degradation reaction were subjected to SDS−PAGE (*33*) and autoradiography. The region of the gel containing ^{125}I-

[1] Abbreviations: βgal, β-galactosidase; BSA, bovine serum albumin; DTT, dithiothreitol; E1, ubiquitin activating enzyme; E2, ubiquitin conjugating enzyme; E3, ubiquitin−protein ligase; H_n, polyHis tract of the indicated number of residues; IPTG, isopropyl β-D-thiogalactopyranoside; NTA, nitrilotriacetic acid; Ubal, ubiquitin aldehyde; Ub_n, polyubiquitin chain composed of *n* ubiquitins; YUH-1, yeast ubiquitin hydrolase-1; one-letter code for amino acids.

lactalbumin conjugates was excised and counted (*24*); the data were corrected by subtracting the counts observed in a comparable incubation lacking ubiquitin. For the supplementation experiments described under Results, E2-14K was purified as described (*31*), and proteins which precipitated from fraction II between 0 and 30% saturation with ammonium sulfate served as the source of E3 (*34*); the latter material was used at a final concentration of 0.4 mg/mL.

Concentration of 26S Proteasomes in Fraction II. Five aliquots of fraction II protein (0.5−20 to μg) were electrophoresed on a 12.5% SDS gel together with four aliquots of purified 26S proteasomes (0.02−2 μg). The gel was blotted, and the blot was developed with polyclonal antibodies directed against subunit S4 of the 19S complex (*35*). Immunocomplexes were detected using alkaline phosphatase-conjugated secondary antibody (BioRad) and colorimetric staining. The S4 signal was approximately equal for 10 μg of fraction II and 2 μg of proteasomes, and for 0.5 μg of fraction II and 0.1 μg of proteasomes (data not shown). Thus, 26S proteasomes comprise ∼20% of the protein in fraction II.

Degradation of ^{125}I-Lysozyme−Ubiquitin Conjugates by the Purified 26S Proteasome. ^{125}I-Lysozyme-H_6−ubiquitin conjugates were prepared and purified as described (*22*), except that bovine serum albumin was added to the Ni−NTA column eluate as a carrier (final concentration, 1 mg/mL). The degradation of the conjugates was monitored by the formation of acid-soluble radioactivity during 10-min incubations (37 °C) with purified 26S proteasomes (*12*) under the following conditions (*22*): 50 mM Tris-HCl (24% base), 5 mM $MgCl_2$, 10% v/v glycerol, 10 mM DTT, 3 μM Ubal, 2 mM ATP, 10 mM phosphocreatine, 0.3 unit/mL creatine phosphokinase, 0.3 unit/mL pyrophosphatase, 0.2−0.37 mg/mL 26S proteasome (0.1−0.2 μM), and ∼5000−8000 cpm of ^{125}I-lysozyme conjugates. Ubal was provided by K. Wilkinson (Emory University) or R. Cohen (University Iowa) (*36*, *37*). Mono-ubiquitin was used as a carrier in these reactions. In some experiments, positive and negative controls were carried out at 3.6 mg/mL mono-ubiquitin, while reactions containing unanchored chains were carried out at 2.4 mg/mL mono-ubiquitin. In most experiments, the total mono-ubiquitin concentration was kept constant at ∼10 mg/mL. Similar results were obtained by both methods, as expected based on the negligible competition by mono-ubiquitin seen in previous studies with this assay (*22*). Data were corrected by subtracting blanks derived from incubations containing unconjugated ^{125}I-lysozyme.

S5a Expression and Purification. Plasmid pET26b−H_{10}−S5a specifies His-tagged human S5a (*38*). The plasmid was transformed into *E. coli* strain BL21(DE3)pLysS. Transformants were grown in 50 mL of LB overnight (37 °C), and these cultures were used to innoculate 4-L cultures, which were grown at 37 °C to A_{600} ∼0.6. IPTG was then added to 0.4 mM. After 4 h more, cells were harvested by centrifugation and lysed as described (*22*). H_{10}−S5a was purified from cell lysates using the His-Bind kit (Novagen). Briefly, lysates were loaded onto a charged 3 mL Ni−NTA column and washed with 30 mL of a buffer containing 5 mM imidazole, 0.5 M NaCl, and 20 mM Tris-HCl, (pH 7.9), followed by a 15-mL wash with the same buffer containing 60 mM imidazole. The tagged S5a was eluted with 1 M imidazole buffer, dialyzed, and concentrated by ultrafiltration. The mutant protein H_{10}-M281T−S5a was similarly expressed and purified. In both cases, about 9 mg of purified S5a was recovered per liter of cell suspension.

Assay of Polyubiquitin Chain Binding to S5a. Binding of unanchored ^{125}I-polyubiquitin chains to purified H_{10}−S5a was carried out as follows. First, 0.25−35 μg of S5a was bound to 5−25 μL of charged Ni−NTA resin (Novagen) in 100 μL of suspension containing 4 M urea, 50 mM Tris (pH 8.0), 0.15 M NaCl, 10 mM imidazole, and 1.3 mg/mL BSA. It was necessary to denature S5a in this step to avoid the formation of S5a−S5a complexes. Suspensions were rotated at RT for 1 h. The resin harboring S5a was then washed 5 times with 300 μL of Tris-buffered saline (50 mM Tris, pH 8.0, 0.15 M NaCl) to remove urea and allow renaturation of S5a. ^{125}I-Labeled polyubiquitin chains at various concentrations were added to S5a resin in up to 200 μL of suspension containing 0.5−3.0 mg/mL BSA and Tris-buffered saline. Suspensions were rotated at 4 °C for 1 h, and then washed once with 300 μL of Tris-buffered saline. The bound radioactivity was quantitated by counting the washed resin pellet in a γ-counter. Data were corrected by subtracting blanks derived from incubations containing the same volume of resin and the same concentration of labeled chains, but lacking S5a. Pilot studies showed that binding was complete within 15 min, and that additional washes did not significantly reduce the amount of bound radioactivity.

RESULTS

Effects of Mutations on Conjugation and Degradation in Reticulocyte Fraction II: Implications for Rate Limitation. We first assessed the ability of each mutant protein to support the ubiquitination and degradation of a well-characterized in vitro substrate, ^{125}I-lactalbumin, in reticulocyte fraction II (*24*). All of the mutant proteins supported degradation, and in all cases degradation was linear with time following a short lag (e.g., Figure 1A). The source of the lag is unknown; it may reflect the time required to build up a significant level of ubiquitin−substrate conjugates. The duration of the lag was independent of the concentrations of DTT and fraction II protein, and did not vary with the identity of residue 8 (Figure 1A and data not shown). Steady-state degradation rates observed with the mutant proteins ranged from 20% (L8G) to 70% (L8I) of the rate seen with wild-type ubiquitin (Figure 1A and Table 1). These rates represent the relative V_{max} values for the respective ubiquitins, because in each case the absolute rate was insenstitive to a 2.7-fold increase in ubiquitin concentration (data not shown). For the series L8G, L8A, L8V, L8I, the rate increased with side chain surface area in a graded fashion; the L8W mutant did not follow this trend (Table 1).

Ubiquitinated forms of ^{125}I-lactalbumin were readily detected in these assays, indicating that all of the mutant proteins were competent in conjugation, as expected based on our previous work (*24*). When the concentration of conjugates was determined at fixed time in the degradative steady-state, the concentration was found to vary with the identity of residue 8, but not in a way that correlated with the rate of proteolysis. In fact, L8G− and L8W−ubiquitin, the two mutants that were most deficient in degradation, gave the highest conjugate levels (Table 1). As shown in Figure

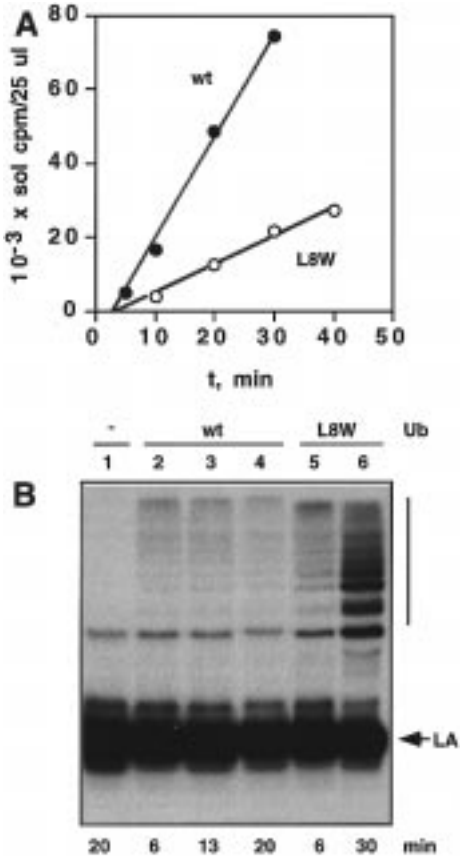

FIGURE 1: Properties of L8W−ubiquitin. (A) Degradation. The production of acid-soluble radioactivity from ^{125}I-bovine lactalbumin (∼300 nM) was assayed in a volume of 150 μL containing 1 mg/mL reticulocyte fraction II protein (Experimental Procedures). The ubiquitin concentration was 12 μM (filled circles, wild-type ubiquitin; open circles, L8W−ubiquitin). (B) Steady-state conjugate level. Aliquots of the degradation assays were removed at the indicated times for determination of the level of ^{125}I-lactalbumin conjugates (Experimental Procedures). Lane 1, no added ubiquitin; lanes 2−4, wild-type ubiquitin (6, 13, and 20 min incubation); lanes 5 and 6, L8W−ubiquitin (6 and 30 min incubation). Bar, region containing ubiquitin−lactalbumin conjugates; LA, unconjugated lactalbumin.

Table 1: Properties of Mutant Ubiquitins: Degradation and Conjugation[a]

mutation	degradation rate (% of wild type)	conjugate level at 14 min (% of wild type)
L8G	19.2 ± 3.7	76.8 ± 9.8
L8A	30.6 ± 4.5	39.7 ± 7.0
L8V	55.6 ± 4.4	51.2 ± 4.3
L8I	70.3 ± 7.9	62.1 ± 3.8
L8W	28.0 ± 2.3	229.0 ± 16.6

[a] Degradation rates and conjugate levels were determined using ^{125}I-bovine lactalbumin in reticulocyte fraction II, at a ubiquitin concentration of 12 μM (Experimental Procedures). Values are mean ± SD of three or more determinations.

1B (lanes 2−4), conjugates assembled from wild-type ubiquitin were present at a constant concentration in the steady-state of degradation; similar results were obtained with L8A−, L8V−, and L8I−ubiquitin (data not shown). In contrast, the concentration of conjugates assembled from L8G− and L8W−ubiquitin increased 2−3-fold during the degradation assay (e.g., Figure 1B, lanes 5 and 6). That the degradation rate was constant while the conjugate concentration increased significantly (compare to open circles, Figure 1A) suggested that the 26S proteasome step was at V_{max} with L8G− and L8W−ubiquitin. This behavior raised the more general question of what step was rate-limiting in the degradation assays. The answer to this question strongly influences the interpretation of the data shown in Table 1 (see below).

To address this issue, we carried out supplementation experiments using wild-type and L8W−ubiquitin. We first used antibodies directed against the S4 subunit of the 19S complex to estimate the concentration of 26S proteasomes in fraction II (Experimental Procedures). The 26S proteasome represented an unexpectedly high fraction, ∼20%, of the protein in fraction II, corresponding to a concentration of 100 nM in the degradation assay. We then doubled the concentration of 26S proteasomes by supplementing the degradation assay with the purified enzyme at 0.2 mg/mL (∼100 nM). There was no effect on the rate observed with either form of ubiquitin (data not shown). (It will be shown below that the purified proteasomes were active in conjugate degradation.) In another set of assays, we simultaneously added purified E1 (140 nM) and E2-14K (30 nM). With both forms of ubiquitin, the rate increased by 50%. In the case of E2-14K, the amount added should have tripled its concentration [cf. 9 nM E2-14K at 1 mg/mL fraction II (*31*)]; the concentration of E1 in fraction II is not known. In a final set of assays, we supplemented with a crude preparation of E3 (*34*). With wild-type ubiquitin, the rate increased by 20−30%; with L8W−ubiquitin, the rate decreased by 20−30%.

The supplementation results indicate that the proteasome-catalyzed step is neither at V_{max} nor rate-limiting in the classical sense, because in either case the degradation rate should have been proportional to the concentration of proteasomes. Supplementing with E1 and E2, which could have an effect by increasing the concentration of conjugates, increased the rate of degradation. This suggests that ubiquitin activation is partially rate-limiting, but this conclusion is at variance with the finding that the degradation rate remained constant despite an increase of >2-fold in the concentration of L8W−ubiquitin conjugates (above). These apparently contradictory results can be reconciled if one assumes that only a small fraction of the conjugates is degraded, and if the concentration of these preferred substrates is constant versus time. These hypothetical good substrates may be the ones bearing the longest chains. Hershko, Rechsteiner and co-workers have shown that the proteasome preferentially degrades highly polyubiquitinated substrates (*39*, *40*), and we have shown that octa-ubiquitin binds to the proteasome 17-fold more tightly than tri-ubiquitin (*22*). We note that in assays with L8W−ubiquitin, it was the level of conjugates bearing three to five ubiquitins which increased most strongly during the assay, whereas the level of the highest molecular weight conjugates remained nearly constant (Figure 1B, lanes 5, 6).

The identity of the rate-limiting step in the degradation assay remains unknown. The supplementation results are generally consistent with partial rate limitation at the stage of ubiquitin activation (and ligation, in the case of wild-type ubiquitin). However, due to the high concentration of proteasomes in the assay, we cannot exclude the possibility that a postrecognition phase of the proteasome reaction is rate-limiting. The concentration of 26S proteasomes, ∼100 nM, definitely exceeded the total concentration of ^{125}I-

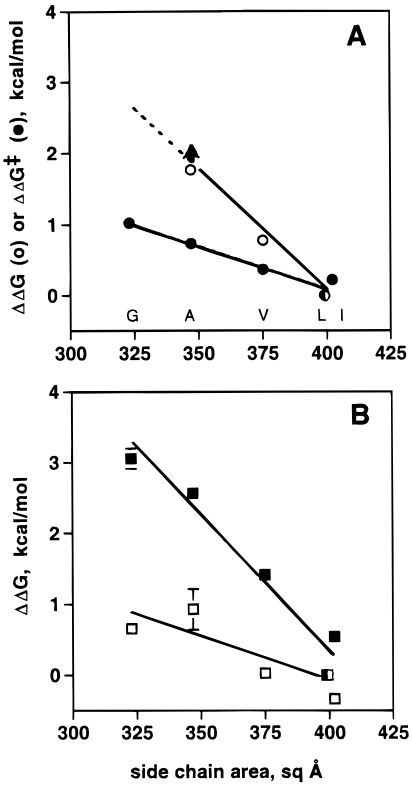

FIGURE 2: Linear free energy diagrams. (A) Reactions involving the 26S proteasome. Relative rates of ubiquitin-dependent degradation in fraction II (filled circles, data from Table 1) and relative inhibition of the purified proteasome by unanchored polyubiquitin chains (open circles, data from Figure 3) were converted to $\Delta\Delta G$ using the relationship: $\Delta\Delta G = -RT \ln(x_{mt}/x_{wt})$, where x_{mt} and x_{wt} are the relevant parameters for mutant and wild-type ubiquitin, and T = 310 K (37 °C). Values of $\Delta\Delta G$ are plotted versus the area of the side chain at residue 8 (*26*). The half-filled circle represents data for wild-type ubiquitin or ubiquitin chains. The arrow indicates that the corresponding point is a lower limit. (B) Binding to S5a. Conversion to $\Delta\Delta G$ was as described in panel A, except $T = 277$ K (4 °C). The filled squares show data for binding to wild-type S5a; the open squares show data for binding to M281T−S5a. Both sets of data are from Table 2. The half-filled square shows data for binding of wild-type ubiquitin chains. Most error bars in both panels are shorter than the diameters of the points.

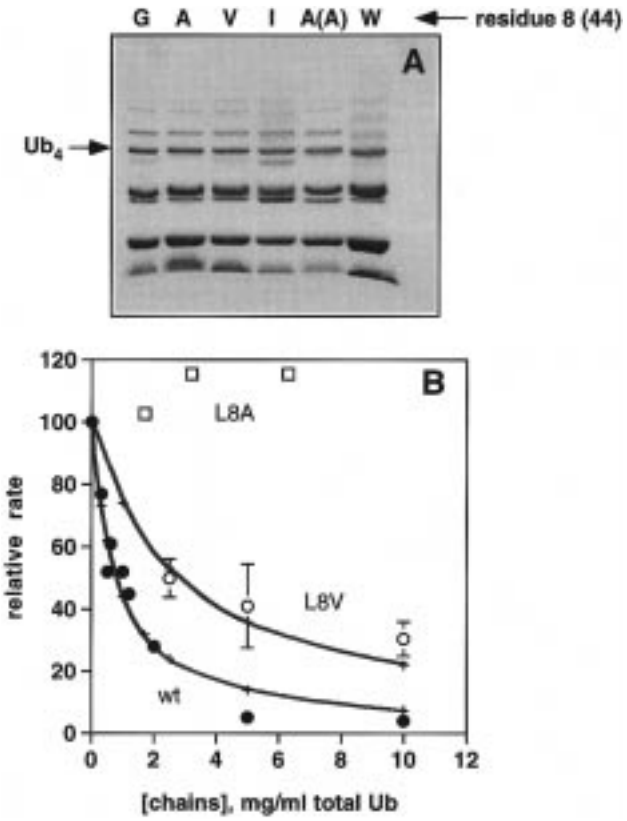

FIGURE 3: Inhibition of 26S proteasomes by unanchored polyubiquitin chains. (A) Polyubiquitin chains (Coomassie-stained gel). Each lane contained ~10 μg of mixed chains assembled from the indicated mutant ubiquitin; the position of Ub_4 is shown. (B) Inhibition of the 26S proteasome. Degradation of purified ^{125}I-lysozyme conjugates by the purified 26S proteasome was assayed (Experimental Procedures) in incubations containing the indicated concentration of wild-type ubiquitin chains (filled circles), L8V−ubiquitin chains (open circles), or L8A−ubiquitin chains (squares). Rates are expressed relative to the rate observed in a control incubation lacking chains. The lines were calculated assuming Michaelis−Menten behavior with $K_{0.5} = 0.8$ mg/mL (filled circles) or $K_{0.5} = 2.8$ mg/mL (open circles). Points with error bars indicate the mean ± SD of three determinations.

lactalbumin conjugates, ≤50 nM (^{125}I-lactalbumin was ~300 nM, and ≤15% of it was conjugated to ubiquitin). The assay also contained an unknown concentration of conjugates derived from fraction II proteins. However, if only a small fraction of conjugates is well-recognized (above), the proteasome may effectively be in "enzyme excess" even if the total concentration of conjugates exceeds the concentration of proteasomes. If the proteasome is in enzyme excess, an internal proteasome step could be rate-limiting for overall degradation. We have previously presented data consistent with rate-limiting conjugate turnover for this substrate (*41*, *42*).

In the present work, the variation in the steady-state degradation rate versus side chain surface area was such that activation energy increased linearly with decreasing area (filled circles, Figure 2A). However, since the rate of ^{125}I-lactalbumin degradation is limited either by conjugate formation or by the turnover of proteasome-bound conjugates (above), this is not a structure−activity correlation for conjugate binding to the proteasome. Consistent with this conclusion, it will be shown below that the filled circles in Figure 2A substantially underestimate the effect of the mutations on conjugate binding to the proteasome.

Effects of Mutations on Polyubiquitin Chain Binding to the 26S Proteasome. To provide an unambiguous measure of the relative interactions of different polyubiquitin chains with the proteasome, we used ubiquitin conjugating enzyme E2−25K to assemble the mutant ubiquitins into unanchored polyubiquitin chains (*43*), and then used the chains to inhibit the degradation of purified ^{125}I-lysozyme conjugates (*22*). Since we were interested in relative rather than absolute affinities, we used mixtures of chains in these assays. The synthetic conditions were adjusted to provide a similar chain length distribution with each mutant ubiquitin; *n* ranged from 1 to ~6, with Ub_2, Ub_3, and Ub_4 as the predominant species (Figure 3A).

Wild-type polyubiquitin chains inhibited the purified proteasome with a saturating concentration dependence which followed $K_{0.5} = 0.8$ mg/mL (filled circles, Figure 3B). This value will correspond to a weighted average of the $K_{0.5}$ values of the different-length chains in the mixture. Based on previous studies with unanchored chains of defined lengths, Ub_4 is expected to be the main inhibitory species (*22*). Figure 3A shows that the level of Ub_4 (and Ub_3) was

comparable among the different mutant chain preparations (this was also true of wild-type chains, data not shown).

Chains assembled from L8V−ubiquitin inhibited 3.5 times more weakly than wild-type chains ($K_{0.5}$ = 2.8 mg/mL; open circles, Figure 3B). Chains assembled from L8A−ubiquitin did not inhibit detectably at concentrations up to 6 mg/mL (open squares, Figure 3B). Assuming that we could have failed to detect 30% inhibition, a lower limit of 14 mg/mL was placed on the value of $K_{0.5}$ for chains assembled from L8A−ubiquitin. Since the inhibition detected in Figure 3 reflects the binding of chains to the proteasome, the stronger effect caused by the L8A and L8V mutations in this experiment, versus Table 1, confirms that chain affinities for the proteasome did not contribute strongly to the rates of ^{125}I-lactalbumin degradation observed in fraction II.

The inability to detect inhibition by L8A−ubiquitin chains precluded an extension of this analysis to the more severely truncating L8G mutation. However, the available data suggest that the dependence of the inhibitory $K_{0.5}$ (Figure 3B) on side chain surface area is much steeper than the dependence shown by the degradation rate in fraction II (open versus filled circles, Figure 2A). As discussed above, this is probably because the rate seen in fraction II is not sensitive to the affinity of chains for the proteasome. In general, the apparent affinities of the mutant chains (open circles, Figure 2A) are consistent with the proposal that the side chain of one or more L8 residues is shielded from solvent when the chain binds to recognition component(s) in the 19S complex (see Discussion).

Effects of Mutations on Chain Binding to S5a. S5a is the only polyubiquitin recognition component thus far identified in the 19S complex. The L8A mutation strongly inhibited chain binding to the 26S proteasome (Figure 3B). We therefore determined how the same mutation affected chain binding to S5a. Since we had already shown that this mutation abolished binding as monitored in the widely used blot overlay method (*24*), it was necessary to develop a more sensitive assay. The new assay employed purified, His-tagged human S5a bound to Ni−NTA resin, with a ^{125}I-polyubiquitin chain(s) as the ligand. As in the blot overlay method (*11*, *19*−*21*), the new assay relies on the slow kinetics of chain dissociation from S5a (Experimental Procedures).

The same chains used for proteasome inhibition studies (Figure 3A) were radiolabeled and used as the "ligand" in the S5a binding studies. As in Figure 3B, the relative affinitites observed in this assay should indicate how the affinity of any given length chain varies as a function of the identity of residue 8. Representative data are shown in Figure 4: binding of wild-type chains was directly proportional to the concentration of S5a, and to the concentration of chains; similar results were obtained in assays with mutant chains (data not shown). Thus, the amount of ligand bound at a fixed concentration of S5a and a fixed concentration of chains was a direct measure of $K_{0.5}$. The data shown in Figure 4 were obtained using a mutant form of S5a (M281T; see below). Comparable results were obtained with wild-type S5a (not shown), except that binding was stronger, so that lower concentrations of S5a could be used.

The relative affinities of the different mutant chains for wild-type S5a are shown in the middle column of Table 2; changes in binding energy with side chain surface area are plotted in Figure 2B (filled squares). The observed linear dependence (Figure 2B) is consistent with a mode of binding in which the hydrophobic effect makes an important contribution; i.e., the side chain of one or more L8 residue is shielded from solvent when a chain binds to S5a (see Discussion).

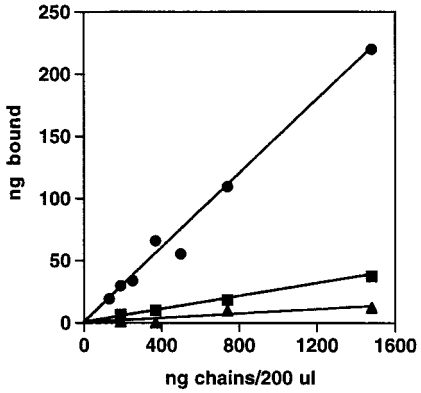

FIGURE 4: Binding of polyubiquitin chains to M281T−S5a. Assays contained the indicated concentration of wild-type ^{125}I-polyubiquitin chains together with 35 μg (circles), 5 μg (squares), or 1 μg (triangles) of H_{10}-M281T−S5a bound to Ni−NTA resin (Experimental Procedures).

Table 2: Binding of Unanchored Polyubiquitin Chains to S5a[a]

mutation	wild-type S5a (% of wild-type chains)	M281T−S5a (% of wild-type chains)
L8G	0.39 ± 0.1	30.3 ± 6.7
L8A	0.95 ± 0.1	18.4 ± 8.8
L8V	7.7 ± 1.6	95.1 ± 17.3
L8I	37.1 ± 5.1	183 ± 13.9
I44A	0.40 ± 0.3	11.9 ± 3.4

[a] Binding of ^{125}I-labeled polyubiquitin chains (see Figure 3A) to H_{10}−S5a bound to Ni−NTA resin was carried out as described under Experimental Procedures. Affinity is expressed relative to the affinity of wild-type polyubiquitin chains determined in the same experiment. Values are mean ± SD of three or more determinations.

M281T Mutation in S5a Alters the Affinity and Specificity of Polyubiquitin Chain Binding. The C-terminal portion of S5a harbors two conserved regions, labeled sites 1 and 2 in Figure 5, which consist of a stretch of hydrophobic residues flanked by charged and polar amino acids. Some of our pilot studies on assay development were carried out with a form of S5a that was subsequently found to harbor a spontaneous Met-to-Thr mutation at the start of the second of these sites (Figure 5). Because this mutation evidently had a strong functional impact, we characterized the mutant protein further. M281T−S5a showed strongly reduced affinity for wild-type polyubiquitin chains (affinity of 6.0 ± 0.3% relative to wild-type S5a, data not shown). This result suggests that site 2 is a chain-binding site. This hypothesis has been confirmed by the results of studies with a synthetic peptide encompassing site 2, and by the results of additional mutagenesis (*44*). A site 1 peptide also binds chains (*44*), consistent with the observation that yeast Mcb1p binds chains (*21*) even though it lacks site 2 (Figure 5).

Besides altering affinity, the M281T mutation altered specificity. Thus, although truncating substitutions at residue 8 reduced binding (Table 2), the dependence of binding on side chain area was less dramatic than the dependence shown by wild-type S5a (open versus filled squares, Figure 2B). There are at least three possible explanations for the altered

```
                                                        1
Hs 181 DALISSPILAGEGGAMLGL.GASD.........F.EFGVDPSADPELALALRVSMEEQRQR
Dm     ---L----Iq--d-.-g-a.-lggnv........-.------ne-----------------
At     -v-L-T-VFT-De--.s-Y.vSAAaaaaaa.ggd-.D-----ni--------------e-a-
Sc     EnIa----IleE-sSgM-af-g-ggdsdan..gt-MD--.---m-----M--------eq--


Hs 231 QEEEARRAAAASAAEAGIATTGTE..................DSDDALLKMTIS.QQEF
Dm     --S-q---npdg-ppT-gdAg-gggvsgsgpgneesagaeneanTEE-M-qrALAlst-t
At     --AAAKK--DeAgqkdkdgd-a-asqetvarttdknaepmd...E-S---dqA-Amsv..
Sc     --rlrqqq.....................................................

                 T      2
Hs 271 GRTGLPDLSSMTEEEQIAYAMQMSLQGAEFGQAESADIDASSAMDTSEPAKEEDDYDVMQ.
Dm     pedn---FAn--------F-----M-d-p.ddSvTqqakrpkTdEAna-mdvDE--seVig
At     GdvnMsEaAD..--qd--L-L---Ms-e-sse-tg-g..................nnLlg
Sc     qqqdq-Eq-EqpEQh-dk*


Hs 331 DPEFLQSVLENLPGVDPNNE.AIRNAMGSLASQATK....DGKKDKKEEDKK*
Dm     --a--------------Qs-e-V-d-V---nk..d-....-k-s-g-Dsq--*
At     nqa-Is---ss-------dp.-VKelLa--pdeskrteeeEsssk-gEDE--*
```

FIGURE 5: S5a sequences. Only the C-terminal portion of the protein is shown (human sequence numbering). Dashes denote identities; dots represent gaps introduced to maximize homology. The bars and numbers indicate two regions that are highly conserved between two or more S5a homologs [*Hs*, human (*38*); *Dm*, *Drosophila* (*51*); *At*, *Arabidopsis* (*20*); *Sc*, yeast (*21*)], and which have been suggested to play a role in polyubiquitin chain binding (*20*, *21*, *38*, *51*).

specificity of M281T−S5a. First, the side chain of M281 could form part of the proposed solvent-shielded site for L8, or M281 could make a van der Waals contact with L8. Second, if the M281T mutation completely inactivates site 2, the specificity shown by M281T−S5a could be that of site 1. In this case, sites 1 and 2 would have related, but distinct, specificities. Since sites 1 and 2 exhibit some cooperativity in chain binding (*44*), a third possibility is that the M281T mutation alters a cooperative interaction between sites 1 and 2. Although further work will be required to distinguish among these possibilities, we favor a model in which the specificity shown by M281T−S5a is that of site 1, because mutational inactivation of site 2 (by multiple Ala substitutions) yields an S5a molecule which binds L8I chains 2-fold better than wild-type chains, as seen for M281T−S5a in Table 2 (P. Young and M. Rechsteiner, unpublished data).

Effect of Chain Length on Binding to S5a. Although one of the most striking features of S5a is its ability to bind long polyubiquitin chains preferentially (*11*, *19*−*21*), the magnitude of this effect has never been accurately measured. We used Ub_4 and Ub_8 generated by a recently developed method (*22*) to address this issue. The method produces chains that are capped at the proximal and distal termini by the presence of a 77th residue (D77) and a K48C mutation, respectively (*22*). We showed in pilot studies that the binding of Ub_4 to S5a was unaffected by the presence of these two modifications: "doubly capped" Ub_4 (bearing both modifications) bound similarly to each of the two singly capped species [in which the distal C48 was alkylated to give *S*-(aminoethyl)-cysteine, or the proximal D77 was removed using the processing enzyme YUH-1; data not shown].

As shown in Figure 6 (squares), ^{125}I-Ub_8 bound to S5a with a saturating concentration dependence that could be fit assuming $K_{0.5} = 1.6 \pm 0.4$ μM, with 1.3 mol of Ub_8/mol of S5a bound at saturation (legend, Figure 6). ^{125}I-Ub_4 also

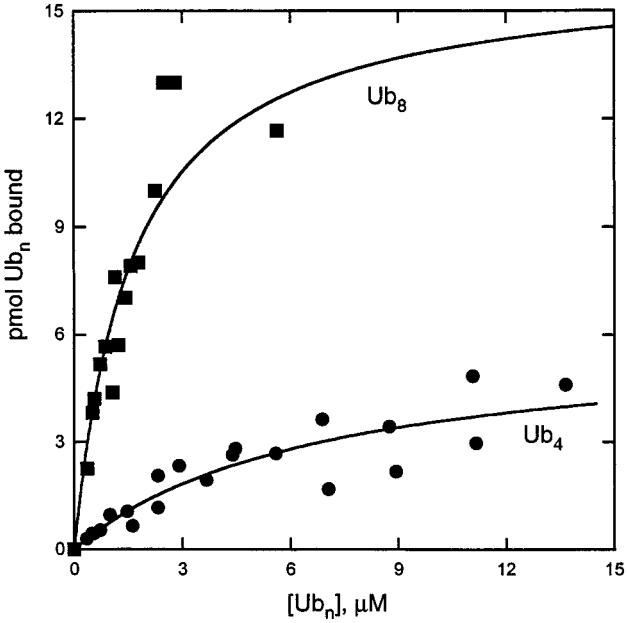

FIGURE 6: Binding of defined-length polyubiquitin chains to wild-type S5a. Binding assays were carried out in incubations of 25 μL containing 6 pmol of H_{10}−S5a (*squares*, Ub_8 binding) or 12 pmol of H_{10}−S5a (circles, Ub_4 binding). Data were normalized to 12 pmol of S5a per incubation. The plot combines data from five independent experiments with each ligand. Data were fit using the program SigmaPlot. For the squares, the line was calculated assuming $K_{0.5} = 1.6 \pm 0.4$ μM and a maximum of 16.1 ± 1.6 pmol bound (1.3 mol of Ub_8/mol of S5a); the point at 5.6 μM represents the mean of triplicate determinations (SD, ±3.58 pmol). For the circles, the line was calculated assuming $K_{0.5} = 6.8 \pm 2.9$ μM, and a maximum of 6.0 ± 1.3 pmol bound (0.57 mol of Ub_4/mol of S5a).

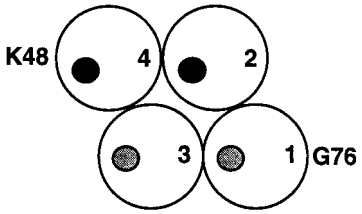

FIGURE 7: Schematic representation of Ub_4 structure (*23*). Each large circle represents one ubiquitin. The ubiquitins are numbered beginning with the proximal ubiquitin in the chain. The small circles represent the hydrophobic patches composed of the side chains of L8, I44, and V70. The solid circles are patches facing the viewer; the stippled circles are patches on the opposite face of the chain.

bound with a saturating concentration dependence, consistent with $K_{0.5} = 6.8 \pm 2.9$ μM (circles, Figure 6). The line fitted to the Ub_4 data assumes a stoichiometry of 0.5 mol of Ub_4/mol of S5a, and the fit is significantly better than that obtained if a 1:1 stoichiometry is assumed (not shown). At present, we can offer no satisfactory explanation for the different apparent binding stoichiometries of Ub_4 and Ub_8.

Two features of the data shown in Figure 6 are noteworthy. First, the 4.2-fold increase in affinity that occurs upon increasing *n* from 4 to 8 (cf. Figure 6) is similar to the factor of 5.8 relating the affinities of the same two chains for the 26S proteasome (*22*). This agreement suggests that the mode of chain binding to the proteasome resembles the mode of binding to isolated S5a (see Discussion). Second, the value of $K_{0.5} = 1.6$ μM for Ub_8 is ~80-fold larger than the value of $K_{0.5} \sim 20$ nM for Ub_7 previously estimated using the blot overlay assay (*11*). The binding of Ub_4 and Ub_8 is also much weaker than expected from our previous results with the blot assay, in which mixed wild-type chains ($n \leq \sim 4$) were saturating at a concentration of 0.6 μg/mL (*22*). Ub_4 was the tightest-binding chain in the mixture. If it had been the only chain present, its concentration would have been ~0.2 μM, leading to the expectation of negligible binding if $K_{0.5}$ was ~7 μM as seen in Figure 6. In fact, Ub_4 was $\ll$0.2 μM in our earlier work, indicating that there is a substantial quantitative difference in the affinities observed in the two assays. It thus appears that the physical state of S5a may strongly influence its properties in chain binding. This is not surprising in view of the recent finding that the chain-binding sites are relatively short stretches of amino acids [Figure 5 (*44*, *45*)]. It is very likely that the degree to which these sites are exposed varies depending upon the physical state of S5a.

DISCUSSION

In the crystal structure of K48-linked Ub_4, a patch composed of the side chains of L8, I44, and V70 forms a repeating feature on two surfaces of the chain [Figure 7 (*23*)]. We showed previously that mutation of pairs of these residues to Ala strongly inhibited degradation mediated by polyubiquitin chains. This conclusion was based primarily on steady-state degradation assays in reticulocyte fraction II, but we also used an in situ version of the assay in Figure 3 to show that chains assembled from L8A,I44A−ubiquitin did not bind detectably to the proteasome (*24*). The same mutations abolished measurable binding of chains to S5a, leading to the suggestion that S5a plays a major role in polyubiquitin chain recognition (*24*). A simple model to accommodate these findings assumes that one or more of the patches on the surface of the chain is shielded from solvent when the chain binds to S5a or other recognition factors in the 19S complex. Such a mode of binding would be entropically favorable (see the Introduction), and might also be favored by van der Waals interactions between side chains in the patch, and nonpolar side chains within the binding site(s).

The current studies were undertaken to address this model for binding, using both the 26S proteasome and isolated S5a. The strategy of successively removing methylene groups from the side chain was based upon mutagenic analyses of protein folding, which indicate that a methylene group contributes 1.2−1.3 kcal/mol in interactions driven by the hydrophobic effect (*25*, *26*). We chose L8 as the site for mutation because among the single mutations analyzed previously, the L8A mutation generated the strongest degradative phenotype in fraction II (*24*). Moreover, the lethality of the L8A mutation in *S. cerevisiae* [cited in (*24*)] indicated a high potential that interactions involving this side chain are functionally relevant.

A Role for the Hydrophobic Effect in Polyubiquitin Chain Recognition. The free energy change associated with the binding of polyubiquitin chains to isolated S5a depended linearly upon the area of the side chain at residue 8 of ubiquitin (filled squares, Figure 2B), as expected if this interaction is driven by the hydrophobic effect. The finding that mutation of Leu to Trp was unfavorable (Table 2) is consistent with expectation for this binding mode; in protein folding, mutation of a small side chain to a larger one is frequently disruptive on steric grounds (*25*, *26*).

The L8A mutation weakened binding by ~3 kcal/mol (Figure 2B). A destabilization of 3.6−3.9 kcal/mol is expected if a single Leu residue goes from full solvent exposure in the unbound state to a completely solvent-shielded environment in the bound state (*25*, *26*). However, inspection of the crystal structures of mono- and tetraubiquitin (*23*, *46)* indicates that only 57% of the side chain of L8 is exposed to solvent (W. Cook, personal communication), leading to a predicted destabilization of 2.1−2.2 kcal/mol for the L8A mutation. The observed destabilization of 3 kcal/mol is significantly larger.

At least two sources may be considered for this extra binding energy. One possibility is that besides the hydrophobic effect, binding is also driven by the formation of favorable van der Waals contacts in the complex. A second possibility is that more than one L8 side chain is buried upon formation of the complex. The observed destabilization of ~3 kcal/mol is fairly close to the ~4 kcal/mol that is expected if two L8 side chains are shielded from solvent upon complex formation. The strong length selectivity shown by S5a [Figure 6 (*11*, *19*, *20*)] is most easily explained by a model in which at least two ubiquitins per chain interact with S5a (see below). However, because S5a could interact differently with these ubiquitins (below), this consideration does not automatically favor a model in which two L8 side chains are shielded during binding.

The robust character of the new S5a binding assay allowed us to monitor binding over a 250-fold range of affinity (Table 2), but the competition assay for chain binding to the proteasome was much less sensitive (Figure 3). Even though it proved impossible to collect data for the full series of

mutants in the latter assay (Results), these data were critical, since we found that the steady-state degradation data (Table 1) significantly underestimated the effects of the mutations on chain binding to the proteasome (Figure 2A, open versus filled circles). The binding data support the mode of interaction discussed above. The L8A mutation destabilized chain binding to the proteasome by >1.8 kcal/mol, and the available data can accommodate a linear dependence of binding energy on side chain surface area (open circles, Figure 2A).

Our results indicate that the hydrophobic effect is important for chain binding to both S5a and the proteasome. We have interpreted this finding in terms of a model in which the side chain of L8 goes from a deshielded to a shielded state upon binding, as a result of interaction with a nonpolar site on (a) recognition component(s). But as discussed previously (*24*), the data do not exclude a model in which the hydrophobic effect is important for maintaining a chain conformation that is necessary for productive binding. In this case, the shielding inferred from our results would involve ubiquitin−ubiquitin contacts. However, only the first model is consistent with the observation that the L8 side chain is similarly surface-exposed in the mono- and tetra-ubiquitin crystals (*23*, *46*). The first model is also consistent with the results of cross-linking experiments, in which chains bearing a reactive group at residue 37 (introduced via a Cys mutation) were found to cross-link efficiently with isolated S5a, and with several subunits of the 19S complex.[2] In the Ub_4 crystal, the side chain of residue 37 is adjacent to the hydrophobic patch (*23*, *24*); the cross-linking results thus suggest that in solution, as in the crystal, this surface of the chain is exposed and accessible to binding components. Nonetheless, confirmation of the molecular interpretation presented above awaits the structural characterization of a complex between a polyubiquitin chain and a bona fide recognition component.

Molecular Basis of Chain Recognition: Elements within the Proteasome. Our results indicate that the side chain of L8 is important for the binding of K48-linked chains both to the 26S proteasome and to S5a. The results further suggest that in both cases, the side chain of L8 makes a favorable contribution to binding as a result of a transition to a solvent-inaccessible environment in the complex. These findings would be most simply explained if S5a plays a major role in polyubiquitin chain recognition at the level of the 26S proteasome.

However, the substantial proteolytic competence of the *mcb1*Δ strain is difficult to reconcile with such a generalized role (*21*). One artificial substrate, Ub-Pro-β-gal, is strongly stabilized in *mcb1*Δ cells, leading to the suggestion that Mcb1p might function in the recognition of a subset of substrates (*21*). In general, substrate-specific phenomena do not exclude the possibility that a particular component plays a generalized role in chain recognition, because such "specificity" can arise from substrate-dependent differences in the identity of the rate-limiting step. However, it can be excluded that the function of S5a in Ub-Pro-β-gal turnover is dependent upon chain binding, because the turnover of this substrate in *mcb1*Δ cells is restored by expression of an S5a derivative which lacks the chain-binding site (*45*).

[2] G. Lawson, D. Finley, and C. Pickart, unpublished experiments.

The role of S5a in the recognition of polyubiquitin chains by the proteasome remains unclear. In vitro studies of 26S proteasomes purified from *mcb1*Δ yeast cells should provide useful evidence on this point. However, our results confirm that S5a provides a valuable model for understanding chain recognition: if currently unidentified factors are indeed the major players in polyubiquitin chain recognition, then these factors must interact with chains rather similarly to S5a.

Our results also bear on a prior inference concerning the existence and properties of non-S5a recognition factors. We reported previously that the I44A and V70A mutations had a much stronger inhibitory effect on chain binding to S5a than on steady-state degradation in fraction II, and suggested that this discrepancy could reflect the presence of other targeting factors, with a lower sensitivity to these mutations (*24*). We have confirmed that the I44A mutation strongly reduces the affinity of chains for S5a [by 250-fold (Table 2)], but we have also shown that the rate of ^{125}I-lactalbumin degradation in fraction II does not reflect the affinity of conjugates for the proteasome (Results). Thus, the divergent results of the two assays do not provide evidence for a proteasomal factor with a binding specificity different from that of S5a.

Molecular Basis of Chain Recognition: Elements within the Chain. We have proposed a model for targeting in which a K48-linked chain creates a unique recognition element that is absent in mono-ubiquitin, and lengthening the chain potentiates targeting by increasing the probability of encountering this element (*22*). We suggested that the hydrophobic patch composed of the side chains of L8, I44, and V70 is a component of the recognition element. The present results confirm this hypothesis in regard to the side chain of L8, and provide information concerning the nature of the interaction involved in its recognition (above). For isolated S5a, the nearby I44 and V70 side chains are also important for recognition [Table 2 (*24*)]. Whether this is also true for the proteasome remains to be determined. However, all of the available data are consistent with a model in which the hydrophobic patch, particularly L8, constitutes an important part of the proposed recognition element.

The length dependence of chain binding to the 26S proteasome (*22*), and to isolated S5a (Figure 6), can be explained by models in which "subsites" on ubiquitins 1 through 4, or ubiquitins 1 and 3, combine to form a minimum recognition element (Figure 7). In both cases, it is predicted that Ub_4 will be the shortest chain to bind efficiently, and Ub_8 will bind 3-fold to 5-fold more tightly than Ub_4 (*22*). The observed differential binding is in approximate agreement with this prediction: 5.8-fold tighter binding of Ub_8 with the 26S proteasome (*22*), and 4.2-fold tighter binding of Ub_8 with isolated S5a (Figure 6). The nature of the proposed minimum recognition element remains to be precisely defined. In the simplest case, there would be only one type of subsite, namely, the hydrophobic patch. However, nothing in the available data excludes the possibility that one or more of the ubiquitins in the proposed minimum element is recognized in a different manner. For example, if subsites on ubiquitins 1 and 3 constitute the minimum element, ubiquitin 1 could interact through its hydrophobic patch, while the interaction with ubiquitin 3 could be electrostatic. Studies involving ubiquitin polymers of defined mutant/wild-type composition, in progress, should help to

clarify the number of subsites in the minimum element, and to discern the types of interactions involved in their recognition.

Implications for Other Targeting Functions of Ubiquitin. The attachment of a single ubiquitin to a membrane protein can be a signal for endocytosis (*47*, *48*). In other cases, mono-ubiquitination apparently modulates substrate assembly into higher-order structures (*49*, *50*). Polyubiquitin chains linked through K63 appear to be involved in nondegradative signaling (*7*, *10*, *48*). Thus, ubiquitination can signal fates other than recognition by the 26S proteasome, and there must exist mechanisms for the selective recognition of certain classes of ubiquitinated proteins. The identity and subcellular localization of the substrate may contribute to such selective recognition. However, the structure and topology of the conjugated ubiquitins may also be important. To the extent that the K48-linked polyubiquitin degradation signal (above) includes side chains of ubiquitin molecules that are not directly covalently linked to each other (e.g., ubiquitins 1 and 3 in Figure 7), the above-discussed model would allow for differential recognition of mono- and di-ubiquitin, versus polyubiquitin chains.

ACKNOWLEDGMENT

We thank Laura Hoffman for a generous gift of 26S proteasomes; Carlos Gorbea for the anti-S4 antibodies; Keith Wilkinson and Bob Cohen for Ubal; and Eileen Kasperek for subcloning the I44A−ubiquitin cDNA. We thank Dan Kosman, Bill Cook, and Bob Cohen for helpful discussions.

REFERENCES

1. Ciechanover, A., Finley, D., and Varshavsky, A. (1984) *Cell 37*, 57−66.
2. Hochstrasser, M. (1996) *Annu. Rev. Genet. 30*, 405−439.
3. Rubin, D. M., and Finley, D. (1995) *Curr. Biol. 5*, 854−858.
4. Shaeffer, J. R. (1994) *J. Biol. Chem. 269*, 29530−29536.
5. Lam, Y. A., Xu, W., DeMartino, G. N., and Cohen, R. E. (1977) *Nature 385*, 737−740.
6. Finley, D., Sadis, S., Monia, B. P., Boucher, P., Ecker, D. J., Crooke, S. T., and Chau, V. (1994) *Mol. Cell. Biol. 14*, 5501−5509.
7. Spence, J., Sadis, S., Haas, A. L., and Finley, D. (1995) *Mol. Cell. Biol. 15*, 1265−1273.
8. Chau, V., Tobias, J. W., Bachmair, A., Marriott, D., Ecker, D. J., Gonda, D. K., and Varshavsky, A. (1989) *Science 243*, 1576−1583.
9. Gregori, L., Poosch, M. S., Cousins, G., and Chau, V. (1990) *J. Biol. Chem. 265*, 8354−8357.
10. Arnason, T., and Ellison, M. J. (1994) *Mol. Cell. Biol. 14*, 7876−7883.
11. Baboshina, O. V., and Haas, A. L. (1996) *J. Biol. Chem. 271*, 2823−2831.
12. Hoffman, L., Pratt, G., and Rechsteiner, M. (1992) *J. Biol. Chem. 267*, 22362−22368.
13. Chu-Ping, M., Vu, J. H., Proske, R. J., Slaughter, C. A., and DeMartino, G. N. (1994) *J. Biol. Chem. 269*, 3539−3547.
14. Löwe, J., Stock, D., Jap, B., Zwickel, P., Baumeister, W., and Huber, R. (1995) *Science 268*, 533−539.
15. Groll, M., Ditzel, L., Löwe, J., Stock, D., Bochtler, M., Bartunik, H. D., and Huber, R. (1997) *Nature 386*, 463−471.
16. Coux, O., Tanaka, K., and Goldberg, A. L. (1996) *Annu. Rev. Biochem. 65*, 801−847.
17. DeMartino, G. N., Moomaw, C. R., Zagnitko, O. P., Proske, R. J., Chu-Ping, M., Afendis, S. J., Swaffield, J. C., and Slaughter, C. A. (1994) *J. Biol. Chem. 269*, 20878−20884.
18. Dubiel, W., Ferrell, K., and Rechsteiner, M. (1995) *Mol. Biol. Rep. 21*, 27−34.
19. Deveraux, Q., Ustrell, V., Pickart, C., and Rechsteiner, M. (1994) *J. Biol. Chem. 269*, 7059−7061.
20. Van Nocker, S., Deveraux, Q., Rechsteiner, M., and Viestra, R. D. (1996) *Proc. Natl. Acad. Sci. U.S.A. 93*, 856−860.
21. Van Nocker, S., Sadis, S., Rubin, D. M., Glickman, M., Fu, H., Coux, O., Wefes, I., Finley, D., and Vierstra, R. D. (1996) *Mol. Cell. Biol. 16*, 6020−6028.
22. Piotrowski, J., Beal, R., Hoffman, L., Wilkinson, K. D., Cohen, R. E., and Pickart, C. M. (1997) *J. Biol. Chem. 272*, 23712−23721.
23. Cook, W. J., Jeffrey, L. C., Kasperek, E. M., and Pickart, C. M. (1994) *J. Mol. Biol. 236*, 601−609.
24. Beal, R., Deveraux, Q., Xia, G., Rechsteiner, M., and Pickart, C. (1996) *Proc. Natl. Acad. Sci. U.S.A. 93*, 861−866.
25. Pace, C. N. (1992) *J. Mol. Biol. 226*, 29−35.
26. Sharp, K. A., Nicholls, A., Friedman, R., and Honig, B. (1991) *Biochemistry 30*, 9686−9697.
27. Burch, T. J., and Haas, A. L. (1994) *Biochemistry 33*, 7300−7308.
28. Li, J., and Pickart, C. M. (1995) *Biochemistry 34*, 15829−15837.
29. Pickart, C. M., Haldeman, M. T., Kasperek, E. M., and Chen, Z. (1992) *J. Biol. Chem. 667*, 14418−14423.
30. Haldeman, M. T., Xia, G., Kasperek, E. M., and Pickart, C. M. (1997) *Biochemistry 36*, 10526−10537.
31. Pickart, C. M., and Vella, A. T. (1988) *J. Biol. Chem. 263*, 12028−12035.
32. Hershko, A., Heller, H., Elias, S., and Ciechanover, A. (1983) *J. Biol. Chem. 258*, 8206−8214.
33. Laemmli, U. K. (1970) *Nature 227*, 680−685.
34. Haas, A. L., and Bright, P. M. (1988) *J. Biol. Chem. 263*, 13258−13267.
35. Richmond, C., Gorbea, C., and Rechsteiner, M. (1997) *J. Biol. Chem. 272*, 13403−13411.
36. Mayer, A. N., and Wilkinson, K. D. (1989) *Biochemistry 28*, 166−172.
37. Dunten, R. L., and Cohen, R. E. (1989) *J. Biol. Chem. 264*, 16739−16747.
38. Ferrell, K., Deveraux, Q., Van Nocker, S., and Rechsteiner, M. (1996) *FEBS Lett. 381*, 143−148.
39. Hershko, A., Leshinsky, E., Ganoth, D., and Heller, H. (1984) *Proc. Natl. Acad. Sci. U.S.A. 81*, 1619−1623.
40. Hough, R., Pratt, G., and Rechsteiner, M. (1986) *J. Biol. Chem. 261*, 2400−2408.
41. Klemperer, N. S., and Pickart, C. M. (1989) *J. Biol. Chem. 264*, 19245−19252.
42. Berleth, E. S., Kasperek, E. M., Grill, S. P., Braunscheidel, J. A., Graziani, L. A., and Pickart, C. M. (1992) *J. Biol. Chem. 267*, 16403−16411.
43. Chen, Z., and Pickart, C. M. (1990) *J. Biol. Chem. 265*, 21835−21842.
44. Young, P., Deveraux, Q., Beal, R. E., Pickart, C. M., and Rechsteiner, M. (1998) *J. Biol. Chem.* (in press).
45. Fu, H., Sadis, S., Rubin, D. M., Gliokman, M., van Nocker, S., Finley, D., and Vierstra, R. D. (1998) *J. Biol. Chem. 273*, 1970−1981.
46. Vijay-Kumar, S., Bugg, C. E., and Cook, W. J. (1987) *J. Mol. Biol. 194*, 531−544.
47. Hicke, L., and Reizman, H. (1996) *Cell 84*, 277−287.
48. Galan, J.-M., and Haguenauer-Tsapis, R. (1997) *EMBO J. 16*, 5847−5854.
49. Busch, H., and Goldknopf, I. L. (1981) *Mol. Cell. Biochem. 840*, 173−187.
50. Ball, E., Karlik, C. C., Beall, C. J., Saville, D. L., Sparrow, J. C., Bullard, B., and Fyrberg, E. A. (1987) *Cell 51*, 221−228.
51. Haracska, L., and Udvardy, A. (1995) *Eur. J. Biochem. 231*, 720−725.

BI972514P